Biological Trace Element Research
https://doi.org/10.1007/s12011-022-03111-y

Gallic Acid and Gallic Acid Nanoparticle Modulate Insulin Secretion Pancreatic β-Islets against Silica Nanoparticle–Induced Oxidative Damage

Akram Ahangarpour[1] · Hassan Sharifinasab[2,3] · Heibatullah Kalantari[2,3] · Mohammad Amin Dehghani[2,3] · Nader Shakiba Maram[4,5] · Fereshteh Golfakhrabadi[6,7]

Received: 29 September 2021 / Accepted: 6 January 2022

Abstract

Due to the increasing use of silica nanoparticles (SiNPs), their possible toxic effects on human health have undoubtedly been considered. Previous studies proved that SiNPs induced oxidative stress. Reactive oxygen species (ROS) and oxidative stress disrupt cell function and decrease insulin secretion. Therefore, this study intended to assess the effects of SiNPs on oxidative stress and insulin secretion and also the protective effects of gallic acid (GA) and gallic acid nanoparticles (NP-GA) on pancreatic β-islets. In this study, the mice islets were separated and pretreated with various concentrations of GA and NP-GA then treated with a single dose of SiNPs. The cell viability of islets examined by MTT assay and also the levels of ROS, malondialdehyde (MDA), glutathione (GSH); activities of superoxide dismutase (SOD), catalase (CAT), glutathione peroxidase (GPx), and insulin secretion were evaluated. The results of MTT assay showed that SiNPs reduced islet viability in a dose-dependent manner and also insulin secretion, induced the formation of ROS, augmented MDA amounts, and decreased GSH levels, SOD, GPx, and CAT activities. Furthermore, pretreatment of islets with GA and NP-GA significantly returned these alterations at low dose. These findings suggested that SiNPs induced oxidative stress in the pancreatic islets, which could be one of the reasons for the decrease in insulin secretion and inducing diabetes. This study also showed that low doses of GA and NP-GA boosted the antioxidant defense system in the pancreatic β-islets, preventing oxidative stress and, consequently, the progression of diabetes.

Keywords Silica nanoparticles · Gallic acid · Gallic acid nanoparticles · Diabetes · Oxidative stress · Islet insulin secretion

✉ Fereshteh Golfakhrabadi
golfakhrabadi@yahoo.com

1 Health Research Institute, Diabetes Research Center, Department of Physiology, Faculty of Medicine, Ahvaz Jundishapur University of Medical Sciences, Ahvaz, Iran

2 Department of Toxicology, School of Pharmacy, Ahvaz Jundishapur University of Medical Sciences, Ahvaz, Iran

3 Toxicology Research Center, Medical Basic Sciences Research Institute, Ahvaz, Iran

4 Nanotechnology Research Center, Ahvaz Jundishapur University of Medical Sciences, Ahvaz, Iran

5 Department of Pharmaceutics, School of Pharmacy, Ahvaz Jundishapur University of Medical Sciences, Ahvaz, Iran

6 Department of Pharmacognosy, Faculty of Pharmacy, Ahvaz Jundishapur University of Medical Sciences, Ahvaz, Iran

7 Medical Basic Sciences Research Institute, Medicinal Plant Research Center, Ahvaz Jundishapur University of Medical Sciences, Ahvaz, Iran

Abbreviations

MDA	Malondialdehyde
GSH	Glutathione
SOD	Superoxide dismutase
CAT	Catalase
GPx	Glutathione peroxidase
ROS	Reactive oxygen species
RNS	Reactive nitrogen species
SiNPs	Silica nanoparticles
GA	Gallic acid
NP-GA	Gallic acid nanoparticles
T2DM	Type 2 diabetes mellitus
TGA	Thermogravimetric analysis
FT-IR	Fourier transform infrared spectroscopy
SEM	Scanning electron microscopy
H2O2	Hydrogen peroxide

Published online: 12 January 2022

Introduction

Mitochondrial respiratory chains are the main source of reactive oxygen species (ROS)/reactive nitrogen species (RNS) in beta cells. The ROS and RNS produced can attack beta cells and cause oxidative damage to them, a process that has been identified in type 2 diabetes mellitus (T2DM). Oxidative stress can cause β-cell dysfunction, insulin resistance, dyslipidemia, impaired glucose tolerance, and T2DM. Chronic oxidative stress is dangerous for β-cells because it stimulates genes involved in apoptosis and cell death [1]. Since the β-cells have little level of antioxidant protection enzymes such as superoxide dismutase (SOD) and catalase (CAT), these cells enormously have excessive sensitivity to free radical–induced impairment [2, 3].

Silica nanoparticles (SiNPs) have been very popular in various industries and biological fields due to their excellent properties such as biocompatibility and biodegradability [4–7]. However, previous assessments have confirmed the SiNPs induced toxicity in human. Several investigations reported increase in ROS production after SiNP exposure in several cell types [8, 9]. It has been shown that amplified ROS levels can lead to the destruction of cytosolic proteins and DNA damage by inducing lipid peroxidation in cell membranes and mitochondria [10]. Consequently, it can be hypothesized that oxidative stress and potential ROS production may be some of the mechanisms of cytotoxicity of SiNP [11]. Given the destructive effects of oxidative stress on the development and progression of T2DM, antioxidant therapy can be considered as a potentially effective method in improving the pathogenesis of T2DM.

Gallic acid (GA) is an isoquinoline alkaloid that is originally extracted from the traditional Chinese plant *Coptis chinensis* (Huang Lian) and is an established treatment for diarrhea in traditional Chinese medicine [11]. Evidence suggests that GA has many biological activities including anti-inflammatory, anti-tumor, immune regulator, hypoglycemic, and hyperlipidemic [12]. GA has shown its protective effect against free radicals as an inhibitor of ROS and reactive nitrogen species. Moreover, GA increases the activity of antioxidant enzymes such as SOD, CAT, glutathione peroxidase (GPx), and glutathione (GSH). Nanostrategies constitute an effective approach to enhance drug delivery across the GA [13].

The use of nanoparticles has been investigated in various studies based on mesoporous silica, polymer, dendrimer, lipid, carbon, and metal nanoparticle platforms to increase bioavailability, and better effectiveness than pure GA has been investigated in various studies [14]. For example, GA nanocapsulation (NP-GA) significantly increased its bioavailability [15] as well as its pharmacological activity [16]. The well-known technique of multiple emulsions and solvent evaporation is commonly used to prepare nanoparticles of hydrophilic drugs. Eudragit RS-100 is a biocompatible polymer with wide application in oral dosage forms.

The aim of this study was to prepare GA nanoparticles with multiple emulsions and solvent evaporation method to increase the efficiency of GA and to investigate the possible protective effect of GA and its nanoparticles on oxidative stress and insulin secretion of pancreatic β-islets against SiNPs toxicity in mice.

Materials and Methods

Chemicals

The SiNPs (length 50–300 nm and diameter 1–2 nm) were obtained from US Research Nanomaterials, Inc. (Houston, TX 77084, USA). 4-(2-Hydroxyethyl)-1-piperazineethanesulfonic acid) (HEPES), mannitol, GA hydrochloride, thiobarbituric acid (TBA), trichloroacetic acid (TCA), ethylene glycol tetraacetic acid (EGTA), 2,7-dichlorofluorescein diacetate (DCFH-DA), bovine serum albumin (BSA), MTT, trichloroacetic acid (TCA), 1,1,3,3-tetramethoxypropane, reduced GSH, oxidized GSH, and Coomassie Brilliant Blue powder were obtained from Sigma-Aldrich (St Louis, Missouri, USA). 5,5-Dithiobis (2-nitrobenzoic acid) (DTNB), dimethyl sulfoxide (DMSO), sodium chloride (NaCl), sodium bicarbonate (NaHCO3), potassium chloride (KCl), calcium chloride (CaCl2), and magnesium chloride (MgCl2) were obtained from Merck company (Darmstadt, Germany). Other required high-purity chemicals were procured from the market.

Animals

The present study was performed on 120 adult male Naval Medical Research Institute (NMRI) mice at the age of 4 to 6 weeks and weighing 20 to 25 g prepared from Ahvaz Jundishapur University of Medical Sciences. The animals were maintained in cages at a controlled temperature (22 + 2 °C) and on a 12:12-h light-dark routine, with free access to drinking water and standard chow. This study was done according to the guidelines of the Animal Ethics Committee of Ahvaz Jundishapur University of Medical Sciences (approval number: IR.AJUMS.REC.1397.036).

Characterization of SiNPs

NP-GA Preparation

NP-GA was prepared using double emulsion-solvent evaporation technique. First, the aqueous phase was prepared by

dissolving 200 mg GA in 30 ml, then the organic phase was obtained by dissolving 400 mg Eudragit RS-100 in 40 ml dichloromethane. For the next step, the aqueous solution was added to the organic phase and became homogenous in an ice bath under homogenization (24,000×*g*), then pre-emulsion (W_1/O) was added to 100 ml polyvinyl alcohol (PVA) (0.2%). Next, the emulsion ($W_1/O/W_2$) was stirred on the magnetic stirrer for 2 h at room temperature; then, suspensions were centrifuged for 30 min at 25 °C (6000×*g*) and separate the supernatant [17].

After the lyophilization of the NP-GA, the production yield was calculated with the following equilibrium:

$$Production\ yield = (Weight\ of\ freeze\ dried\ nanoparticles\ (mg)\ )/(Weight\ of\ drug\ (mg) + Polymer\ (mg)) \times 100 \quad (1)$$

The production yield experiments were carried out three times and the statistical analysis was done.

NP-GA suspension was centrifuged at 6000×*g* for 30 min at 25 °C, then 10 ml of the supernatant containing unloaded GA was placed in the dialysis bag. The bag was then placed in a becher containing 20 ml of PBS. The becher was stirred on a magnetic stirrer for 30 min (50×*g*) at room temperature to let the solutions become equilibrated with each other. Finally, the absorption of unloaded GA was measured by spectrophotometry, Shimadzu spectrophotometer (Kyoto, Japan) at 420 nm. Entrapment efficiency (EE %) was calculated using the following formula:

$$EE\% = (amount\ of\ drug\ in\ the\ formulation\ (mg) - amount\ of\ unloaded\ drug\ in\ supernatant\ (mg))/(amount\ of\ drug\ in\ the\ formulation\ (mg)\ ) \times 100 \quad (2)$$

Nanoparticle Size Analysis

Prior to the experiment, NP-GA was first diluted with double distilled water and then the particle size was analyzed using a particle size analysis tool (Scatteroscope 1 Qudix, Korea). Each test was performed three times and the average of three numbers was calculated as the final result [17].

SEM

Surface morphology of NP-GA was determined by SEM (Leo 1455 VP, Germany). Two milligrams of the NP-GA suspension was poured onto an aluminum sheet to dry at room temperature, then coated with a 50 nm gold/palladium alloy, and finally the surface morphology of the nanoparticles was studied [17].

FT-IR

To reveal the probable interactions between drug and polymer, infrared spectroscopy of the formulation, drug and Eudragit RS were carried out by IR spectroscope equipment (vortex 70, Bruker, Germany) using KBr disk over a range of 500–4000 cm^{-1} [17].

Zeta Potential

A zeta seizer measuring device was used to examine the surface charge of nanoparticles (Malvern, ZEN3600, UK). Nanoparticles were suspended in distilled water (pH = 7) at 25 °C. The surface charge test was carried out three times, and the average of the measurements was reported as zeta potential [18].

TGA of SiNPs

The thermograms of the drug and formulation were recorded on Chromatopac R6A Thermal Analyzer (Shimadzu, Japan). Five milligrams of nanoparticles, GA, and Eudragit RS-100 were transferred separately to aluminum pans, and the samples were scanned from 50 to 1150 °C at the heating rate of 10 °C/min using an empty aluminum pan as reference [17].

Dissolution Studies

The in vitro release profile of GA from the polymeric nanoparticles was studied by the dialysis bag diffusion technique under sink condition for formulations. The dialysis bag retained nanoparticles and allowed the diffusion of the drug immediately into the recipient compartment. Eighty milligrams of lyophilized nanoparticles was added to 10 ml of PBS and stimulated the intestinal medium in the dialysis bag and placed in 20 ml of dissolution medium in a water bath on a heater with a magnetic stirrer, and the temperature was kept at 37 ± 1 °C, then stirred at 50 rpm. The dialysis bag was removed from the becher at 0.5-, 1-, 2-, 4-, 6-, 8-, 12-, and 24-h intervals and placed in a new one containing 20 ml of fresh buffer. The sample's volume was reduced to 5 ml by rotary (Heidolph, 4EF63CX- 4, Germany), then their UV absorption was measured by the spectrophotometer. The UV absorption of the solutions was read at 420 nm [17].

Dispersion of SiNPs

The SiNPs were dispersed in distilled water; then, 600 mcg of stock suspensions to reduce agglomeration was mixed by vortex for 20 s and sonicated for 20 s by a sonicator probe (ultrasonic processor VCX-750 W, Vibra-Cell™). The stock

suspensions were then diluted with distilled water and sonicated as before to prepare test concentrate [17].

Isolation of Islets

The mice pancreatic islets were isolated by collagenase digestion method. In short, after dislocating the neck, the animals' bellies are opened. The bile duct was closed at the distal end near the duodenum. Then, 5 ml of Hank's Balanced Salt Solution (HBSS) including NaCl 115 mmol/l, NaH_2PO4 1.2 mmol/l, HEPES 25 mmol/l, D-glucose 5 mmol/l, NaHCO3 10 mmol/l, KCl 5 mmol/l, MgCl2 1.1 mmol/l, CaCl2 2.5 mmol/l, BSA 1%, and collagenase P 1.4 mg/ml with PH: 7.4 were injected into the duct. The pancreas were removed and placed into a tube and incubated at 37 °C water bath for 15 min. Then, 15 ml of cold HBSS was added to the tube containing pancreas to dilute collagen and end the enzymatic digestion progression. To remove the collagenase from islet tissues, the tubes containing pancreas were centrifuged and supernatant rejected. The islets were washed three times and the sediment containing the islets was transferred to Petri dish. The islets were isolated under a stereomicroscope and cultured in RPMI-1640 medium along with 100 U/ml penicillin, 10% fetal bovine serum, 5 mM D-glucose, and 100 U/mL streptomycin and was subjected with 95% O2 to 5% CO2 atmosphere.

Insulin Secretion Measurement

Insulin secretion was assessed in a glucose static incubation. The separated islets were divided into 36 groups (10 islets in each group); 12 groups for concentration of 2.8 mM of glucose +12 groups for concentration of 5.6 mM of glucose +12 groups for concentrations of 16.7 mM of glucose. After the end of the treatment, islets were washed and incubated at 37 °C for 1 h with concentrations of 2.8 mM, 5.6 mM, and 16.7 mM of glucose. Next, islets were centrifuged at 3500 rpm for 15 min and the supernatants were collected and insulin concentration was measured by a Rat Insulin ELISA (Monobind, USA). The results were reported with µU/islet/h [19].

Group I: Control group; islets were cultured in RPMI-1640 medium for 48 h.
Group II: H_2O_2 group; islets were cultured for 24 h in RPMI medium then exposed with H_2O_2 (50 µM) for 2 h [19].
Group III: SiNP group alone; islets were cultured for 24 h in RPMI medium then exposed with 240 µg of SiNPs for 24 h [19].
Group IV: Islets were pretreated with 10 µg of glibenclamide (GLIB) for 24 h and then exposed with 240 µg of SiNPs for 24 h [19].
Group V: Islets were pretreated with 7.5 µM of GA for 24 h and then exposed with 240 µg of SiNPs for 24 h.
Group VI: Islets were pretreated with 20 µM of GA for 24 h and then exposed with 240 µg of SiNPs for 24 h.
Group VII: Islets were pretreated with 40 µM of GA for 24 h and then exposed with 240 µg of SiNPs for 24 h.
Group VIII: Islets were pretreated with 7.5 µg of NP-GA in RPMI medium for 24 h then exposed with 240 µg of SiNPs for 24 h.
Group IX: Islets were pretreated with 20 µg of NP-GA in RPMI medium for 24 h then exposed with 240 µg of SiNPs for 24 h.
Group X: Islets were pretreated with 40 µg of NP-GA in RPMI medium for 24 h then exposed with 240 µg of SiNPs for 24 h.
Group XI: Islets were treated with 40 µg of GA in RPMI medium for 48 h.
Group XII: Islets were treated with 40 µg of NP-GA in RPMI medium for 48 h [19].

Islet's Viability Evaluation

The islet's viability was calculated by MTT test after islet's exposure with different concentrations of GA and NP-GA against 240 µg of SiNPs by the ELISA Kit. Concisely, pretreated islets were washed twice by Krebs-HEPES buffer; after washing, MTT solution (20 µl) was added to pretreated islets and incubated at 37 °C for 4 h. Then, DMSO (100 µl) was added to tests and the absorbance of samples was read at 570 nm. The islet viability of the control group was considered as 100% and the rest of the groups were calculated accordingly [20].

Islet Preparation for Biochemical Tests

For biochemical analysis, 50 islets in each group were selected. Then, the islets were washed three times with ice-cold PBS and lysed through sonication for 10 s (ultrasonic processor VCX-750 W); then, homogenated solution was centrifuged for 10 min at 4 °C. The obtained supernatant was used to measure the biochemical tests [21].

MDA, GSH, GPx, CAT, and SOD Measurement

GSH, SOD, GPx, and CAT protect the cell against ROS damage and free radicals. During lipid peroxidation, free radicals damage cell membranes by oxidative degradation of lipids.

GPx plays an important role in preventing the lipid peroxidation process and consequently protects cells from oxidative stress. The GPx activity was estimated by quantifying the rate of oxidation of the reduced GSH to the oxidized GSH by H2O2 catalyzed by GPx. The GPx kit (ZellBio

GmbH, Lonsee, Germany) utilizes an enzymatic recycling method based on the reaction between GSH and 5,5-dithiobis (2-nitrobenzoic acid) (DTNB) that produces a yellow colored compound (NBT). The GPx activity was measured at 412 nm by Shimadzu spectrophotometer (UV-1650PC SHIMADZU**,** Kyoto, Japan) [22].

SOD enzyme activity was identified by the ZellBio kit (ZellBio GmbH, Lonsee, Germany). In summary, in this protocol, the xanthine-xanthine oxidase agent was used as a superoxide anion producer and caused the reduction of nitroblutotrazolium composition to formazan dye. Then, SOD enzyme activity was assessed based on superoxide radical inhibition according to manufacture method and was measured by spectrophotometer (UV-1650PC SHIMADZU, Kyoto, Japan) at 505 nm.

To determine the level of MDA, the liver tissue homogenate was mixed with TCA then centrifuged for 5 min and TBA reagent added to supernatant, then was incubated in a hot water bath for 30 min. After cooling, the absorbance was recorded at 532 nm by Shimadzu spectrophotometer (UV-1650PC SHIMADZU**,** Kyoto, Japan) [23].

To determine CAT activity, the supernatant was mixed with phosphate buffer (pH: 7.5) then hydrogen peroxide (30 mM) was added to this mixture to begin the reaction. The rate of H2O2 decomposition was assessed by measuring the absorbance changes at 240 nm for 1 min. One unit of CAT activity was defined as 1 mM of H2O2 that was consumed in 1 min and was measured by Shimadzu spectrophotometer (UV-1650PC SHIMADZU**,** Kyoto, Japan); ultimately, the specific activity of CAT was expressed as unit per milligram of protein [22]**.**

To determine of the GSH level, the liver homogenate was mixed with phosphate buffer (pH: 7.5) and TCA (50%) for 15 min, then centrifuged at room temperature for 15 min at 2000 g to precipitate tissue proteins. The supernatant was mixed with Tris buffer (0.4 M) at pH 9.8 and 0.01 M 5,5′-dithiobis (2-nitrobenzoic acid) solution (DTNB), and the absorption was read at 412-nm Shimadzu spectrophotometer (UV-1650PC SHIMADZU**,** Kyoto, Japan). The result was expressed as micromoles of GSH per milligrams of protein [23].

ROS Evaluation

To evaluate the amount of ROS, fluorometric assay and DCFH-DA fluorescent material were used. Concisely, pretreated groups of islets were washed with PBS, then DCFH-DA (40 µM) solution was added to samples and incubated for 30 min. In the next step, the islets were washed with PBS, lysed with NaOH, and centrifugated for 10 min at 4 °C and the obtained supernatant was used to measure the fluorescence of dichlorofluorescein. Finally the light absorbance of samples was read by fluorescence spectrophotometer (F-7000, Hitachi, Japan) with excitation 485-nm and emission 530-nm wavelengths. The fluorescence intensity of the control group was considered as 100%, and the rest of the treatment groups were calculated as a percentage of control group [24].

Protein Calculation

The amount of protein in islet tissue was measured by Bradford method [25]. The pretreated islets were first prepared according to the groups mentioned above. After centrifugation, 1 ml of Bradford prepared solution was poured onto 20 µl of supernatant in each tube. Then, the light absorbance of samples was read at 595 nm. BSA solution was prepared as standard.

Statistical Analysis

The results of this study were statistically analyzed using GraphPad Prism (version 5.04). Data were considered as mean ± standard deviation (SD) by one-way analysis of variance (ANOVA) followed by post hoc Tukey's test. The statistical differences were considered significantly at $p < 0.05$.

Results

Production Efficiency

The preparation of nanoparticles was done with different methods, such as high-pressure homogenization, solvent evaporation methods, solvent diffusion, emulsification, and high-shear homogenization. However, the method used in this study was based on microemulsion with organic solvents. The production efficiency of the formulation is shown in Table 1; the production efficiency of NP-GA was measured 85.15% ± 4.37 that was an acceptable loading efficiency for prepared nanoparticles.

Loading Yield

As shown in Table 1, the loading yield of the formulation was estimated to be 94%, which was an acceptable loading yield of the formulation. It was possible that as the ratio of polymer to drug increased, more particles of the drug were

Table 1 The production efficiency, loading yield, mean particle size, and PDI

Mean production efficiency ± SD (%)	Mean loading yield ± SD (%)	Mean particle size mean ± SD (nm)	Mean PDI ± SD
85.15% ± 4.37	94%	169 ± 14.9	0.26 ± 0.014

trapped inside the nanoparticles. When the homogenizer speed changed, no significant difference in loading efficiency was observed [26].

Particle Size

As observed in Table 1 and Fig. 1, the average of polydispersity index and particle size formulation, meant particle size was 169 nm. One study similar to this investigation described that particle size with Eudragit RS-100:drug ratio was 1:1 and 3:1. As observed in Table 1, the polydispersity index (PDI) of formulation was 0.26 that could be acceptable for polymer-based nanoparticles [27].

SEM

The results of this study based on SEM images exhibited that the nanoparticles had a spherical surface and were comparatively uniformed (Fig. 2). Because of this, the pharmacokinetics of nanoparticles in the body are somewhat more predictable.

FT-IR

The results of this study based on the FT-IR spectrum displayed a peak at 1722 cm^{-1}, which showed the presence of a polymer in the nanoparticle due to its carbonyl-ester group; existence peaks at 1469–1653 cm^{-1} (aromatic ring) in the nanoparticle approved loaded drug on nanoparticle. The results of IR spectra showed shift of the stretch ester carbonyl stretching peak of the amine salt groups at 2950–2988 cm^{-1} and peak of stretching C-H at 3433 cm^{-1}in GA. The decrease in the intensity of the mentioned peaks was due to the interaction between the drug and the polymer. Hydrogen binding interactions between drug and polymer could stabilize both the drug and the polymer that this issue was also reported by Adibkia et al. [27]. Spectrum of nanoparticles showed the presence of the following characteristic peaks: C = O stretching at 1637 cm^{-1}. The complete disappearance of the GA characteristic peak at 1646 cm^{-1} in inclusion complexes

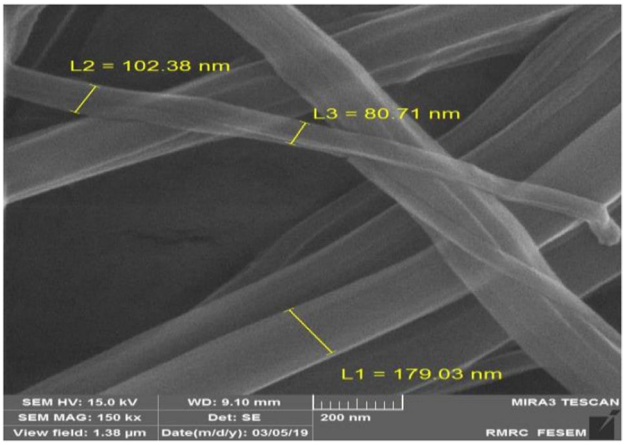

Fig. 2 SEM images of GA

could be attributed to the inclusion of functional groups of GA into the nanoparticles. Probably, because of the attraction of the polymer steric oxygen by the hydroxyl groups of GA, the stretching peak at 1752 cm^{-1} was related to the shifted carbonyl group peak in Eudragit RS-100 and drug which shifted to the higher wavelength presenting the strengthening of this bond because of increased polarity.

Zeta Potential

The zeta potential of formulation +30.5, pure drug −40.8, and pure polymer +40.3 were detected. Because the surface charge of Eudragit RS-100 was positive, drug-polymer encapsulation revealed a uniform polymer coating by SEM imaging. The measured zeta potential was sufficient to stabilize and prevent the accumulation of nanoparticles [28].

TGA

The analysis of TGA showed that the regents were heated from 50 to 1150 °C in air atmosphere at 10 °C/min. The sharp

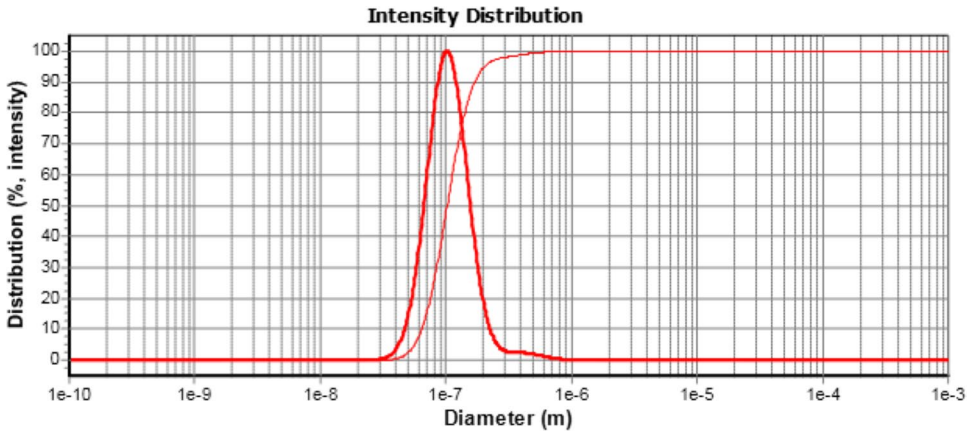

Fig. 1 Size distribution of NP-GA

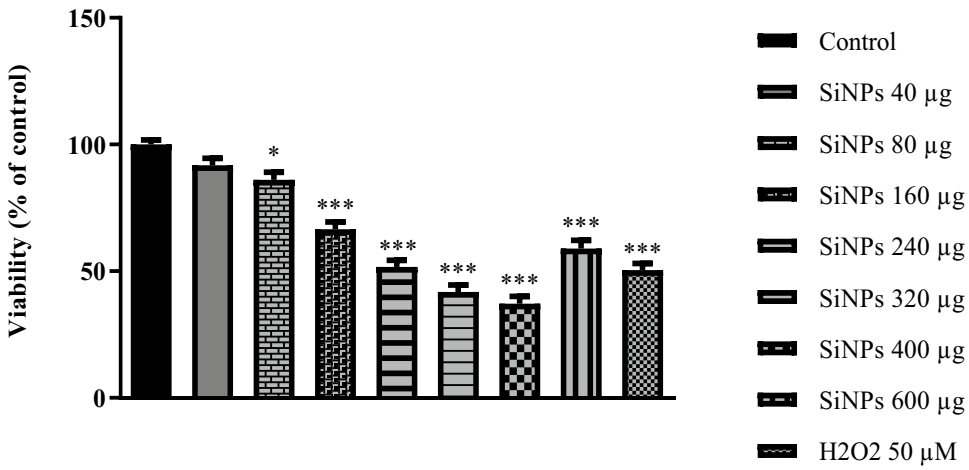

Fig. 3 Effects of SiNP treatment on the viability of isolated mice islets. Islets were exposed to SiNPs (40, 80, 160, 240, 320, 400, and 600 µg) for 24 h or H2O2 50 µM for 2 h, and then cell viability was measured (7 mice in each group). The difference between the control and other groups was significant at $p < 0.05$ (*), $p < 0.01$ (**), and $p < 0.001$ (***). SiNPs, silica nanoparticles; H2O2, hydrogen peroxide

peak at 146 °C was observed in the thermograms of drug and formulation that associated with the melting point of the drug. The presence of the polymer in the formulation made this peak shorter in association with the pure drug and the higher ratio of polymer lead to a shorter peak. The percentage of the drug thermal decomposition decreased in formulation. This designates the thermal stability of the drug in the presence of the polymer, triggering the stability of the ready formulation.

Dissolution Examination in PBS

According to the data, approximately 20% of the initial drug was released in 30 min. In solvent evaporation, diffusion occurs in almost all microspheres [29]. Probably due to particle surface erosion, the release of the GA near the nanoparticle surface by electrostatic attraction was an explosive emission. Various data have shown that insufficient drug release was common when solvent evaporation was used. One study described the inadequate ibuprofen release from the Eudragit RS-100 microspheres ready by solvent evaporation method, which was probably due to drug-polymer interactions and/or the delay property of the polymer [30, 31]. Another possibility was less swelling of the Eudragit RS-100 after absorption of the dissolution medium and reduction of drug release with water absorption due to hydrogen bond interactions. The mechanism of drug release was according to logarithmic Wagner type.

Response-Dose of SiNPs

First, the islets were pretreated with different doses of SiNPs (40, 80, 160, 240, 320, 400, and 600 µg) for 24 h, then cell viability was evaluated by MTT test. To calculate islets viability, the control group considered 100% and the rest of the treatment and pretreatment groups were compared to the control group. When islets were treated with 240, 320, or 400 µg of SiNPs, cell viability was reduced by about 50% ($p < 0.001$). Therefore, 240-µg dose was selected as the optimal dose (Fig. 3).

Effect of GA and NP-GA on Cell Viability in SiNP-Treated Islets

After obtaining the optimal dose in 24 h, first, the islets were pretreated with different doses of GA (7.5, 20, and 40 µM) and NP-GA (7.5, 20, and 40 µM) then treated with 240 µg of SiNPs. As shown in Fig. 4, pretreated islets with 7.5 and

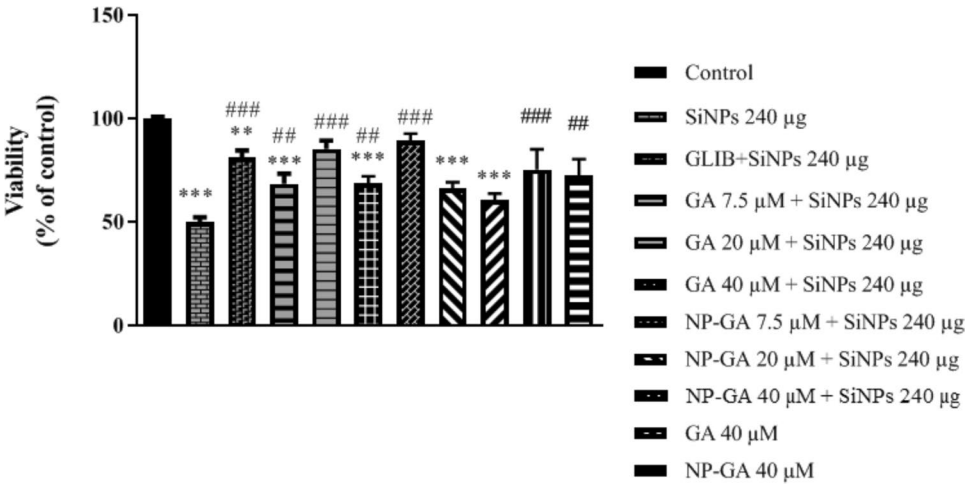

Fig. 4 Pretreatment islets with GA (7.5, 20, and 40 µM), NP-GA (7.5, 20, and 40 µM), and glibenclamide (GLIB, 10 µM) for 24 h and then treatment with SiNPs (240 µg) for 24 h for cell viability evaluation. The difference between control and other groups was significant at $p < 0.01$ (**) and $p < 0.001$ (***). The difference between SiNPs and other groups was significant at $p < 0.01$ (##) and $p < 0.001$ (###). SiNPs, single-walled carbon nanotube; GA, gallic acid; NP-GA, gallic acid nanoparticle; GLIB, glibenclamide

20 and 40 µM of GA as well as 7.5 µM of NP-GA meaningfully augmented the cell viability ($P<0.01$, $P<0.001$). But, there was no important alteration in cell viability of NP-GA 20 and 40 µM + 240 µg of SiNPs in comparison with the control group after 24 h.

Effect of GA and NP-GA on Insulin Secretion in SiNP-Treated Islets

As shown in Fig. 5A, 2.8 mM of glucose significantly increased the insulin secretion in GA (20 µM) and NP-GA (7.5 µM) plus 240 µg of SiNPs groups ($P<0.05$ and $P<0.01$). As shown in Fig. 5B, 5.6 mM of glucose significantly increased the insulin secretion in GA (7.5 and 20 µM) and NP-GA (7.5 µM) plus 240 µg of SiNPs groups ($P<0.05$, $P<0.01$ and $P<0.001$). However, as shown in Fig. 5C, 16.7 mM of glucose significantly increased the insulin secretion in GA (7.5, 20, and 40 µM) and NP-GA (7.5 and 20 µM) plus 240 µg of SiNPs groups ($P<0.05$ and $P<0.01$ and $P<0.001$).

Effect of GA and NP-GA on SOD Activity in SiNP-Treated Islets

In all concentrations of glucose medium, SOD activity of islet significantly decreased in SiNP group alone compared to the control group ($P<0.001$). In 2.8- and 5.6-mM glucose medium, SOD activity significantly improved in GA 7.5 and 20 µM ($P<0.05$, $P<0.001$) as well as NP-GA 7.5 µM ($p<0.001$) and glibenclamide 10 µM ($P<0.01$) groups compared to SiNP group alone (Tables 2 and 3).

In 16.7-mM glucose-containing medium, only a protective effect was observed in the GA 20 µM ($P<0.001$), NP-GA 7.5 µM ($P<0.001$), and glibenclamide 10 µM ($P<0.01$) groups compared to SiNP group alone (Table 4).

Effect of GA and NP-GA on GSH Levels in SiNP-Treated Islets

As shown in Tables 2, 3, and 4, GSH levels displayed a significant decrease in SiNP group alone compared to the control group ($P<0.001$), while in all concentrations of glucose in 24-h treatment of islets, 7.5 and 20 µM of GA, 7.5 µM of NP-GA, and glibenclamide 10 µM significantly improved GSH levels compared to SiNP group alone ($P<0.05$, $P<0.01$, $P<0.001$).

Effect of GA and NP-GA on GPx Activity in SiNP-Treated Islets

According to our results, after the addition of SiNP to the islets, the GPx activity of islet significantly decreased compared to the control group in all concentrations of glucose medium ($P<0.001$), while in concentrations of 2.8- and 16.7-mM glucose medium; GPx activity significantly improved by GA 20 µM, NP-GA 7.5 µM, and glibenclamide 10 µM groups compared to SiNP group alone ($P<0.05$, $P<0.01$, and $P<0.001$) (Tables 2 and 4). But, in concentration of 5.6-mM glucose medium, GPx activity significantly improved by GA 7.5 and 20 µM, NP-GA 7.5 µM, and glibenclamide 10 µM groups compared to SiNP group alone ($P<0.05$, $P<0.01$, and $P<0.001$) (Table 3).

Fig. 5 Pretreatment islets of GA (7.5, 20, and 40 µM), NP-GA (7.5, 20, and 40 µM) and glibenclamide (GLIB, 10 µM) for 24 h and then treatment with SiNPs (240 µg) for 24 h for insulin secretion calculation and a subsequent 1-h incubation with **a** 2.8 mM, **b** 5.6 mM, or **c** 16.7 mM glucose-containing medium. Results are expressed as mean ± SD. The difference between control and other groups is significant at $p<0.01$ (**) and $p<0.001$ (***). The difference between SiNPs and other groups is significant at $p<0.05$ (#) and $p<0.01$ (##) and $p<0.001$ (###). SiNPs, silica nanoparticles; SEM, standard error of mean; GA, gallic acid; NP-GA, gallic acid nanoparticle; GLIB, glibenclamide

Effect of GA and NP-GA on MDA Levels in SiNP-Treated Islets

In all concentrations of glucose medium, after incubation of islets with 240 µg of SiNPs, the MDA levels significantly augmented compared to the control group ($P<0.001$). Furthermore, the MDA level of islets with 7.5 and 20 and 40 µM of GA, 7.5 µM of NP-GA and glibenclamide 10 µM significantly decreased compared to SiNPs group alone ($P<0.05$, $P<0.01$, and $P<0.001$) (Tables 2, 3 and 4).

Effect of GA and NP- GA on CAT Activity in SiNPs -Treated Islets

According to our results, after the addition of SiNPs to the islets, the CAT activity of islet significantly decreased compared to the control group in all concentrations of glucose medium ($P<0.001$). In concentrations of 2.8- and 5.6-mM glucose medium, a remarkable increase in CAT activity was observed in 7.5 and 20 µM of GA ($P<0.05$ and $P<0.001$), 7.5 µM of NP-GA ($P<0.001$) and glibenclamide 10 µM ($P<0.01$) compared to the SiNPs group alone (Tables 2, 3, and 4). In concentration of 16.7-mM glucose medium, a significant increase in CAT activity was observed in 40 µM of GA ($P<0.05$) compared to the SiNP group alone (Table 4).

Effect of GA and NP-GA on ROS Levels in SiNP-Treated Islets

As shown in Fig. 6, the exposure of islets to SiNPs significantly increased the production of ROS compared to the

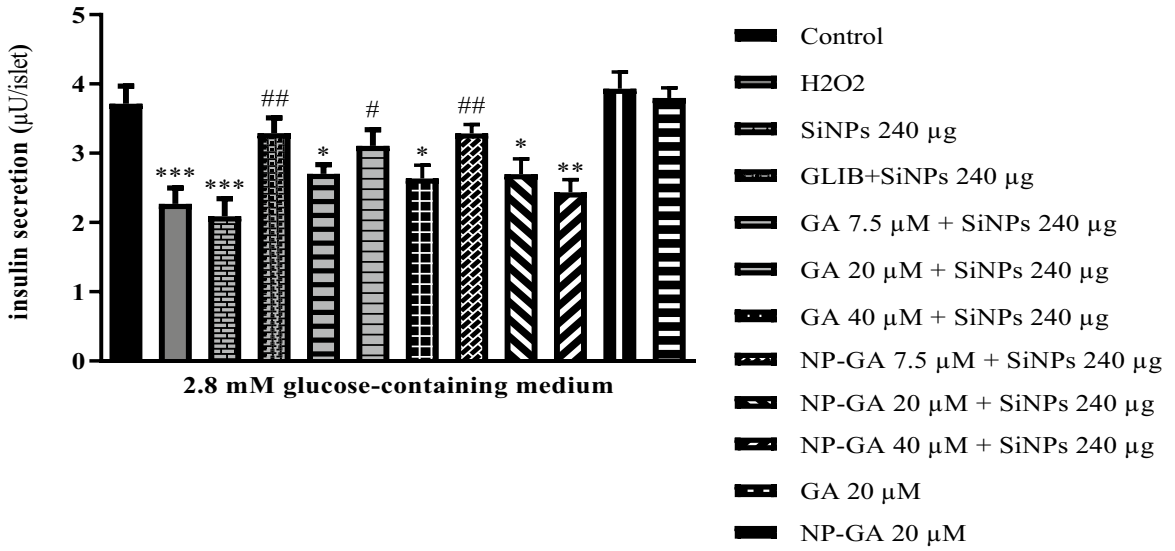
insulin secretion (μU/islet)
2.8 mM glucose-containing medium
Control
H2O2
SiNPs 240 μg
GLIB+SiNPs 240 μg
GA 7.5 μM + SiNPs 240 μg
GA 20 μM + SiNPs 240 μg
GA 40 μM + SiNPs 240 μg
NP-GA 7.5 μM + SiNPs 240 μg
NP-GA 20 μM + SiNPs 240 μg
NP-GA 40 μM + SiNPs 240 μg
GA 20 μM
NP-GA 20 μM

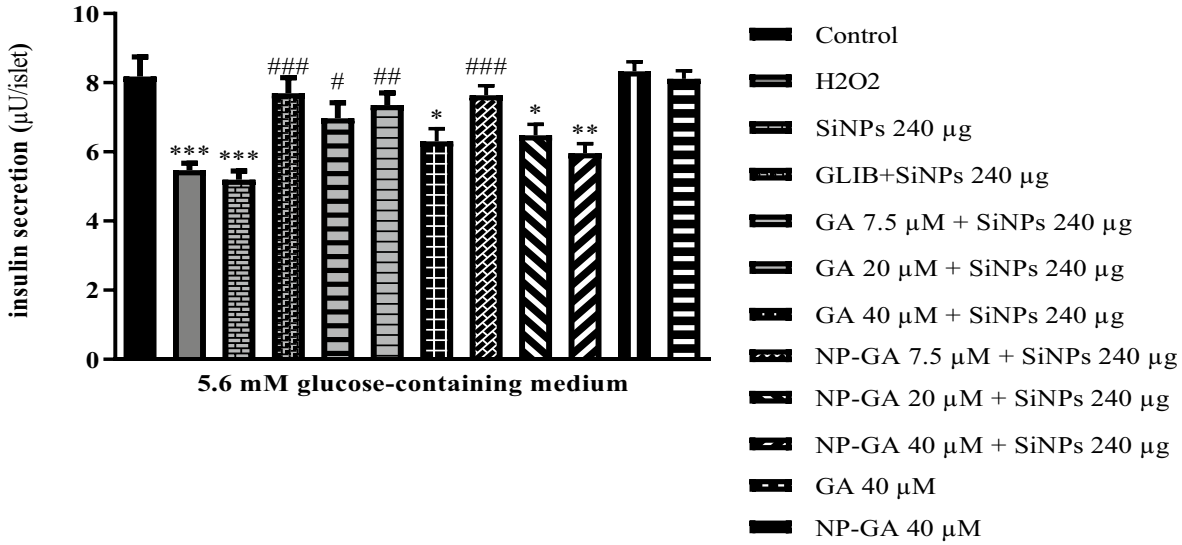
insulin secretion (μU/islet)
5.6 mM glucose-containing medium
Control
H2O2
SiNPs 240 μg
GLIB+SiNPs 240 μg
GA 7.5 μM + SiNPs 240 μg
GA 20 μM + SiNPs 240 μg
GA 40 μM + SiNPs 240 μg
NP-GA 7.5 μM + SiNPs 240 μg
NP-GA 20 μM + SiNPs 240 μg
NP-GA 40 μM + SiNPs 240 μg
GA 40 μM
NP-GA 40 μM

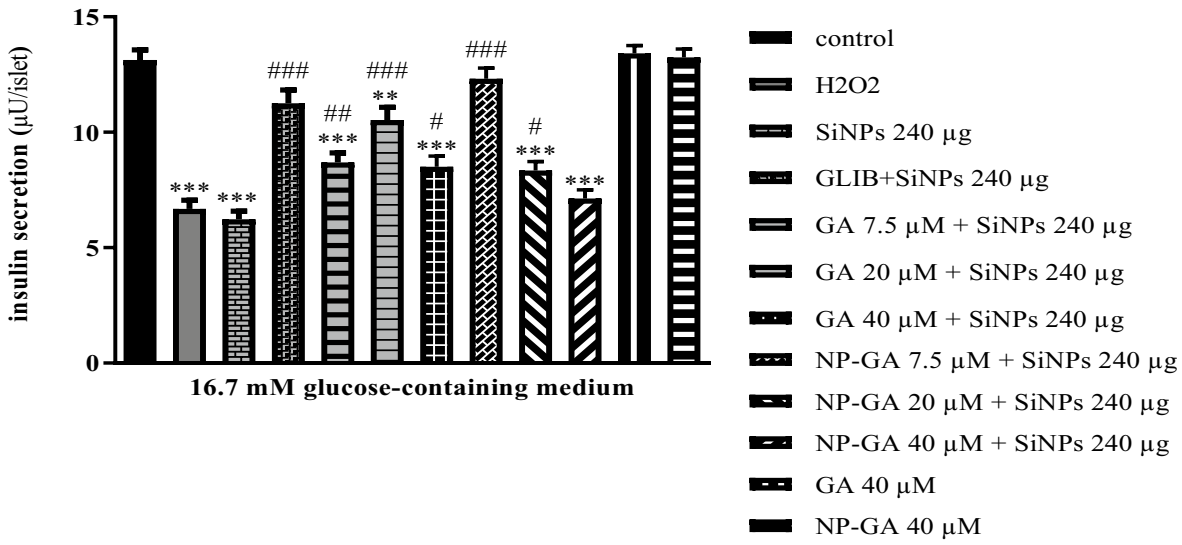
insulin secretion (μU/islet)
16.7 mM glucose-containing medium
control
H2O2
SiNPs 240 μg
GLIB+SiNPs 240 μg
GA 7.5 μM + SiNPs 240 μg
GA 20 μM + SiNPs 240 μg
GA 40 μM + SiNPs 240 μg
NP-GA 7.5 μM + SiNPs 240 μg
NP-GA 20 μM + SiNPs 240 μg
NP-GA 40 μM + SiNPs 240 μg
GA 40 μM
NP-GA 40 μM

Table 2 Pretreatment islets with GA (7.5, 20, and 40 µM), NP-GA (7.5, 20, and 40 µM) and glibenclamide (GLIB, 10 µM) for 24 h and then treatment with SiNPs (240 µg) for 24 h and a subsequent 1-h incubation with 2.8-µM glucose-containing medium

Groups	GSH (mg/mg protein)	MDA (nmol/mg protein)	CAT (U/mg protein)	SOD (U/mg protein)	GPx (U/mg protein)
Control	59.60 ± 3.24	6.34 ± 0.74	4.59 ± 0.48	40.06 ± 3.75	102.10 ± 6.64
SiNP 240 µg	29.77 ± 2.94 *	9.96 ± 1.10 *	1.95 ± 0.18 *	18.55 ± 3.34 *	75.50 v 6.32 *
SiNP 240 + GLIB 10 µM	48.29 ± 5.39 ###	7.88 ± 1.16 ###	3.06 ± 0.46 ##	28.44 ± 3.70 ##	90.09 ± 6.46 ##
SiNP 240 + GA 7.5 µM	41.39 ± 4.67 ##	8.09 ± 0.84 ##	2.85 ± 0.42 #	26.36 ± 3. 67b #	86.83 ± 6.11
SiNP 240 + GA 20 µM	47.93 + 4.92 ###	7.15 v 0.69 ###	3.21 ± 0.42 ###	30.35 ± 5.69 ###	90.72 ± 5.56 #
SiNP 240 + GA 40 µM	40.37 + 6.94 #	8.27 ± 1.02 #	2.77 ± 0.45	25.67 ± 3.87	84.57 ± 5.95
SiNP 240 + NP-GA 7.5 µM	50.80 ± 6.35 ###	7.07 ± 0.92 ###	3.76 ± 0.45 ###	34.60 ± 3.52 ###	93.78 ± 5.60 ###
SiNP 240 + NP-GA 20 µM	38.74 ± 4.56	8.38 ± 0.46	2.65 ± 0.40	25.36 ± 3.54	83.36 ± 6.93
SiNP 240 + NP-GA 40 µM	35.09 ± 5.20	8.85 ± 0.75	2.27 ± 0.37	22.71 ± 3.56	81.02 ± 5.68
GA 40 µM	64.31 ± 3.83	6.49 ± 0.57	4.92 ± 0.47	43.06 ± 4.26	105.20 ± 7.36
NP-GA 40 µM	61.30 ± 4.78	6.32 ± 0.64	4.75 ± 0.60	41.15 ± 4.88	103.70 ± 6.46

Values expressed as mean ± SD

*$P < 0.001$ significant difference from the control group

# $P < 0.05$, ## $P < 0.01$, and ### $P < 0.001$ significant differences from the SINP group

Table 3 Pretreatment islets with GA (7.5, 20, and 40 µM), NP-GA (7.5, 20, and 40 µM) and glibenclamide (GLIB, 10 µM) for 24 h and then treatment with SiNPs (240 µg) for 24 h and a subsequent 1-h incubation with 5.6-µM glucose-containing medium

Groups	GSH (mg/mg protein)	MDA (nmol/mg protein)	CAT (U/mg protein)	SOD (U/mg protein)	GPx (U/mg protein)
Control	61.54 ± 3.14	5.10 ± 0.71	4.95 ± 0.65	42.88 ± 4.10	105.7 ± 8.00
SiNP 240 µg	33.09 ± 3.71 *	10.04 ± 0.89 *	2.26 ± 0.36 *	20.86 ± 3.62 *	79.15 ± 6.09 *
SiNP 240 + GLIB 10 µM	50.60 ± 5.54 ###	6.81 ± 0.59 ###	3.71 ± 0.46 ##	31.54 ± 6.15 ##	92.46 ± 5.89 ##
SiNP 240 + GA 7.5 µM	44.52 ± 5.31 ##	8.08 ± 0.93 ##	3.35 ± 0.40 #	29.63 ± 3.37 #	89.69 ± 5.96 #
SiNP 240 + GA 20 µM	49.26 ± 5.05 ###	6.70 ± 0.65 ###	3.95 ± 0.58 ###	32.94 ± 3.21 ###	93.30 ± 6.73 ##
SiNP 240 + GA 40 µM	44.17 ± 3.32 ##	8.16 ± 1.03 ##	3.15 ± 0.40	28.06 ± 3.27	88.78 ± 4.90
SiNP 240 + NP-GA 7.5 µM	53.90 ± 4.25 ###	6.12 ± 0.50 ###	4.15 ± 0.40 ###	36.15 ± 3.80 ###	96.53 ± 5.36 ###
SiNP 240 + NP-GA 20 µM	42.40 ± 5.36 #	8.36 ± 0.60 #	3.05 ± 0.53	27.44 ± 4.30	87.43 ± 5.05
SiNP 240 + NP-GA 40 µM	38.96 ± 5.58	8.83 ± 0.89	2.72 ± 0.62	25.35 ± 3.29	85.21 ± 4.19
GA 40 µM	55.98 ± 7.73	6.87 ± 0.75	3.63 ± 0.41	36.02 ± 4.51	97.20 ± 6.12
NP-GA 40 µM	48.77 ± 6.50	7.12 ± 0.53	3.39 ± 0.47	30.52 ± 3.50	93.86 ± 7.41

Values expressed as mean ± SD

*$P < 0.001$ significant difference from the control group

# $P < 0.05$, ## $P < 0.01$, and ### $P < 0.001$ significant differences from the SINPs group

control group ($P < 0.001$). However, pretreatment islets with 7.5, 20, and 40 µM of GA ($P < 0.05$, $P < 0.01$, and $P < 0.05$, respectively) and 7.5 and 20 µM of NP-GA ($p < 0.001$ and 0.05, respectively) significantly inhibited SiNP-induced ROS production.

Discussion

The data of this study demonstrated that SiNPs induced oxidative stress, reduced insulin secretion in pancreatic β-islets, and possibly caused diabetes. Pretreatment islets with GA (7.5 and 20 µM) and NP-GA (7.5 µM) significantly ameliorated oxidative stress factors including ROS, MDA, GSH, SOD, GPx, and CAT and increased insulin secretion.

NP-GA was obtained by double emulsion-solvent evaporation method using Eudragit RS 100 as a polymer and polyvinyl alcohol as carrier. The data of this study established that this method was appropriate for the preparation of NP-GA by evaluation zeta potential, size, dispersity, morphology, drug release studies, and thermal gravimetric analysis of nanoparticles. According to previous studies on the biocompatibility of Eudragit RS-100 and its widespread application in oral formulations, its use for the preparation of GA nanoparticles was confirmed with double emulsion and solvent evaporation [32, 33]. In agreement with our study, one study reported that quercetin nanoparticles were

Table 4 Pretreatment islets with GA (7.5, 20, and 40 μM), NP-GA (7.5, 20, and 40 μM) and glibenclamide (GLIB, 10 μM) for 24 h and then treatment with SiNPs (240 μg) for 24 h and a subsequent 1-h incubation with 16.7-μM glucose-containing medium

Groups	GSH (mg/mg protein)	MDA (nmol/mg protein)	CAT (U/mg protein)	SOD (U/mg protein)	GPx (U/mg protein)
Control	56.89 ± 5.00	7.31 ± 0.64	4.32 ± 0.49	37.72 ± 3.19	98.52 ± 5.32
SiNP 240 μg	25.47 ± 6.25 *	12.34 ± 1.02 *	1.51 ± 0.47 *	17.62 ± 3.05 *	72.91 ± 5.94 *
SiNP 240 + GLIB 10 μM	41.40 ± 7.40 ##	10. 29 ± 0.82 ##	2.82 ± 0.36 ###	26.54 ± 3.57 ##	86.81 ± 7.20 ##
SiNP 240 + GA 7.5 μM	37.41 ± 5.08 #	10.48 ± 0. 89 #	2.56 ± 0.30 ##	23.76 ± 2.98	83.04 ± 4.18
SiNP 240 + GA 20 μM	43.10 ± 5.30 ###	9.34 ± 0.87 ###	2.98 ± 0.53 ###	28.24 ± 3.40 ###	87.36 ± 5.01 ##
SiNP 240 + GA 40 μM	36.43 ± 7.38 #	10.64 ± 0.86 #	2.35 ± 0.29 #	24.03 ± 4.49 d #	82.47 ± 5.71
SiNP 240 + NP-GA 7.5 μM	49.17 ± 4.45 ###	8.24 ± 0.79 ###	3.41 ± 0.42 ###	32.53 ± 3.79 ###	91.06 ± 5.78 ###
SiNP 240 + NP-GA 20 μM	34.73 ± 5.07	10.71 ± 0.93	2.31 ± 0.23 #	23.05 ± 2.75	81.70 ± 4.50
SiNP 240 + NP-GA 40 μM	32.73 ± 5.55	11.09 ± 1.05	2.17 ± 0.21	20.94 ± 2.76	78.68 ± 4.02
GA 40 μM	48.47 ± 4.20	7.50 ± 0.59	3.55 ± 0.84	35.85 ± 4.75	96.20 ± 7.00
NP-GA 40 μM	37.81 ± 4.39 d	8.05 ± 0.55	3.26 ± 0.53	30.37 ± 4.67	92.70 ± 6.18

Values expressed as mean ± SD

*$P < 0.001$ significant difference from the control group

# $P < 0.05$, ## $P < 0.01$, and ### $P < 0.001$ significant differences from the SINPs group

prepared by nanoprecipitation technique with Eudragit E and polyvinyl alcohol and the results showed that antioxidant activity of quercetin nanoparticles was more than pure quercetin [34]. Previous studies have performed the manufacture of nanoparticles to increase their antioxidant properties and increase their penetration into cells. In this regard, Vico et al. reported the SiNP formulation with GA [35] and Kim et al. reported the synthesis of gold nanoparticles using GA as a capping agent [36].

Studies have shown that SiNPs induce oxidant stress and ROS production. Oxidative stress increases the accumulation of ROS. In physiological conditions, ROS levels are controlled by the balance between ROS production and its elimination by the cellular antioxidant system including GSH, SOD, GPx, and CAT. SiNPs produce free radicals such as superoxide anion, hydrogen peroxide, and hydroxyl radicals that react with the cellular membrane lipids and cause lipid peroxidation. The MDA is the end product of lipid peroxidation [37–39]. In this study, SiNPs significantly increased islets' MDA and ROS levels and reduced islets' GSH levels compared to the control group which also significantly decreased islets' CAT, GPx, and SOD activities. While GA (7.5 and 20 μM) and NP-GA (7.5 μM) significantly reduced MDA and ROS levels and increased the GSH levels, CAT, SOD and GPx activity in islets.

One study found that SiNP vasodilate aorta, which was blocked by the antioxidant enzyme SOD. Improving the vasodilation induced by SiNPs with SOD indicated the involvement

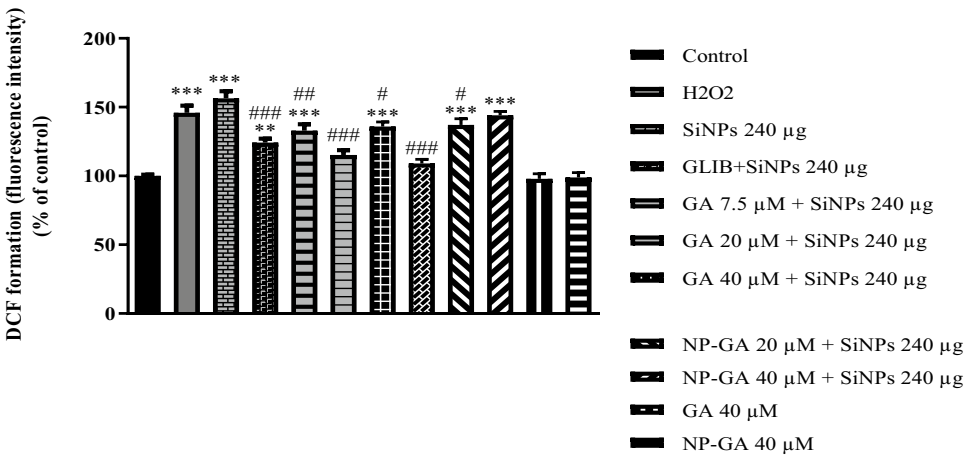

Fig. 6 Pretreatment islets with GA (7.5, 20, and 40 μM), NP-GA (7.5, 20, and 40 μM) and glibenclamide (GLIB, 10 μM) for 24 h and then treatment with SiNPs (240 μg) for 24 h for reactive oxygen species estimation. Results are expressed as mean ± SD. The difference between control and other groups is significant at $p < 0.01$ (**) and $p < 0.001$ (***). The difference between SiNPs and other groups is significant at $p < 0.05$ (#) and $p < 0.01$ (##) and $p < 0.001$ (###). SiNPs, silica nanoparticles; SEM, standard error of mean; GA, gallic acid; NP-GA, gallic acid nanoparticle; GLIB, glibenclamide

of oxidative stress mechanism in this toxicity [40]. In the same line, one study reported that SiNPs induced endothelial dysfunction through mitochondrial dynamics and change of biogenesis [41]. Another study showed that the accumulation of ROS in pancreatic β cells caused them to lose their proper function [42].

In this study, the islets' exposure to SiNPs significantly reduced the insulin secretion after the addition of 2.8, 5.6, and 16.7 mM of glucose mediums. Due to the vulnerability of pancreatic islets to oxidative damage and low levels of antioxidants in this tissue, their contact to ROS can stimulate some cellular stress-sensitive ways which are associated with reduced insulin secretion. It seems to be a relationship between K_{ATP} current and β-cell function in cases of mild oxidative stress. Low levels of ROS help β-cell function and the regulation of insulin gene expression. While high levels of ROS reduce insulin gene expression and insulin secretion, it leads to islet disorder. The three factors of glucose metabolism, ROS production, and ATP production as a result of K_{ATP} channel activity are associated with β-cell dysfunction. Increased SiNPs impair ATP production and open K_{ATP} channels, leading to hyperpolarization of β-cells to limit calcium influx and glucose-induced insulin secretion. Mitochondrial ROS accumulation followed by ATP depletion is associated with metabolism and cell death [19, 43]. Our findings have shown that SiNPs as inducers of ROS reduced the insulin secretion of pancreatic islets by generating the oxidative stress.

GA is well-known as a natural antioxidant involved in both inhibitory and scavenging actions of ROS [44]. GA was also reported the increased activity of antioxidant enzymes such as SOD, GPx, and glutathione S-transferase with a simultaneous reduction in amounts of ROS in lymphocytes without any modification in the total antioxidant capacity [45]. Cells treated with high glucose exhibited a significant rise in mRNA expression of TNFα, IL-6, NADPH oxidase, and TXNIP; all these changes were weakened in the presence of GA. High glucose levels also increase SOCS-3 expression while GA can regulate this effect [46]. GA could also rise insulin secretion in β- cells and up-regulate mRNA of PDX-1 and insulin [47]. Also the results of one study showed that GA and NP-GA with their potential antioxidants could improve renal mitochondrial dysfunction, oxidative stress, and inflammation in cisplatin-induced nephrotoxicity in rat [17]. The antioxidant properties of GA and its nanoparticles are probably due to the phenolic hydroxyl groups present in their molecular structure.

Conclusion

The findings of this study showed that GA and its nanoparticles improved insulin secretion and oxidative stress induced by SiNPs in Langerhans β-islets in mice. The present study also demonstrated that NP-GA was successfully produced by double emulsion-solvent evaporation method and established their properties. GA (7.5 and 20 μM) and NP-GA (7.5 μg) significantly ameliorated insulin secretion and the amounts of ROS, MDA, GSH, SOD, GPx, and CAT. Finally, GA and its nanoparticles can be considered as potential antioxidants in alternative therapy for diabetes in cases where the toxic agents act on the oxidative stress mechanism. However, more detailed molecular studies, including studies of other mechanisms involved in Langerhans islets injury and the development of diabetes, are needed to evaluate the efficacy of these compounds for future clinical use.

Funding This study was supported by a grant from the Department of Pharmacognosy, Faculty of Pharmacy, Ahvaz Jundishapur University of Medical Sciences, Ahvaz, Iran.

Declarations

Approval was obtained from the ethics committee of Ahvaz Jundishapur University of Medical Sciences (AJUMS.REC.1398.636). All the participants were informed of the aims of the study, and informed consents were obtained from them.

Conflict of Interest The authors declare no competing interests.

References

1. Tangvarasittichai S (2015) Oxidative stress, insulin resistance, dyslipidemia and type 2 diabetes mellitus. World J Diabetes 6:456–480
2. Wolf G, Aumann N, Michalska M, Bast A, Sonnemann J, Beck JF (2010) Peroxiredoxin III protects pancreatic ss cells from apoptosis. J Endocrinol 207:163–175
3. Vessby J, Basu S, Mohsen R, Berne C, Vessby B (2002) Oxidative stress and antioxidant status in type 1 diabetes mellitus. J Intern Med 251:69–76
4. Wang Y, Zhao Q, Han N, Bai L, Li J, Liu J (2015) Mesoporous silica nanoparticles in drug delivery and biomedical applications. Nanomedicine 11:313–327
5. Mebert AM, Baglole CJ, Desimone MF, Maysinger D (2017) Nanoengineered silica: properties, applications and toxicity. Food Chem Toxicol 109:753–770
6. Castillo RR, Colilla M, Vallet-Regi M (2017) Advances in mesoporous silica-based nanocarriers for co-delivery and combination therapy against cancer. Expert Opin Drug Deliv 14:229–243
7. Kurtz-Chalot A, Villiers C, Pourchez J, Boudard D, Martini M, Marche PN (2017) Impact of silica nanoparticle surface chemistry on protein corona formation and consequential interactions with biological cells. Mater Sci Eng C Mater Biol Appl 75:16–24
8. Gilardino A, Catalano F, Ruffinatti FA, Alberto G, Nilius B, Antoniotti S (2015) Interaction of SiO2 nanoparticles with neuronal cells: ionic mechanisms involved in the perturbation of calcium homeostasis. Int J Biochem Cell Biol 66:101–111
9. Guo C, Yang M, Jing L, Wang J, Yu Y, Li Y (2016) Amorphous silica nanoparticles trigger vascular endothelial cell injury through apoptosis and autophagy via reactive oxygen species-mediated MAPK/Bcl-2 and PI3K/Akt/mTOR signaling. Int J Nanomedicine 11:5257–5276

10. Marks DBM, A.D., Smith CM (1996) Oxygen metabolism and oxygen toxicity. In Basic Medical Biochemistry: A Clinical Approach
11. Ceriello A, Testa R (2009) Antioxidant anti-inflammatory treatment in type 2 diabetes. Diabetes Care 32:dc09–S316
12. Johansen JS, Harris AK, Rychly DJ, Ergul A (2005) Oxidative stress and the use of antioxidants in diabetes: linking basic science to clinical practice. Cardiovasc Diabetol 4:1475–2840
13. Tillhon M, Guaman Ortiz LM, Lombardi P, Scovassi AI (2012) Berberine: new perspectives for old remedies. Biochem Pharmacol 84:1260–1267
14. Chen X, Zhang Y, Zhu Z, Liu H, Guo H, Xiong C (2016) Protective effect of berberine on doxorubicininduced acute hepatorenal toxicity in rats. Mol Med Rep 13:3953–3960
15. Poupot R, Bergozza D, Fruchon S (2018) Nanoparticle-based strategies to treat neuro-inflammation. Materials:11
16. Mirhadi E, Rezaee M, Malaekeh-Nikouei B (2018) Nano strategies for berberine delivery, a natural alkaloid of Berberis. Biomed Pharmacother 104:465–473
17. Dehghani MA, Maram NS, Moghimipour E, Khorsandi L, Mahdavinia M (2020) Protective effect of gallic acid and gallic acid-loaded Eudragit-RS 100 nanoparticles on cisplatin-induced mitochondrial dysfunction and inflammation in rat kidney. Biochim Biophys Acta Mol basis Dis 1866:165911
18. Zhang W, Li X, Ye T, Chen F, Yu S, Chen J (2014) Nanostructured lipid carrier surface modified with Eudragit RS 100 and its potential ophthalmic functions. Int J Nanomedicine 9:4305
19. Ahangarpour A, Alboghobeish S, Oroojan AA, Dehghani MA (2018) Mice pancreatic islets protection from oxidative stress induced by single-walled carbon nanotubes through naringin. Hum Exp Toxicol 1(960327118769704):0960327118769704
20. Hosseini A, Baeeri M, Rahimifard M, Navaei-Nigjeh M, Mohammadirad A, Pourkhalili N (2013) Antiapoptotic effects of cerium oxide and yttrium oxide nanoparticles in isolated rat pancreatic islets. Hum Exp Toxicol 32:544–553
21. Xiong F-L, Sun X-H, Gan L, Yang X-L, Xu H-B (2006) Puerarin protects rat pancreatic islets from damage by hydrogen peroxide. Eur J Pharmacol 529:1–7
22. Shokrzadeh M, Bagheri A, Ghassemi-Barghi N, Rahmanian N, Eskandani M (2021) Doxorubicin and doxorubicin-loaded nanoliposome induce senescence by enhancing oxidative stress, hepatotoxicity, and in vivo genotoxicity in male Wistar rats. Naunyn Schmiedeberg's Arch Pharmacol 394:1803–1813
23. Armann B, Hanson M, Hatch E (2007) Quantification of basal and stimulated ROS levels as predictors of islet potency and function. Am J Transplant 7:38–47
24. Ahangarpour A, Oroojan AA, Rezae M, Khodayar MJ, Alboghobeish S, Zeinvand M (2017) Effects of butyric acid and arsenic on isolated pancreatic islets and liver mitochondria of male mouse. Gastroenterol Hepatol Bed Bench 10:44
25. Bradford MM (1976) A rapid and sensitive method for the quantitation of microgram quantities of protein utilizing the principle of protein-dye binding. Anal Biochem 72:248–254
26. Nath B, Nath LK, Kumar P (2011) Preparation and in vitro dissolution profile of zidovudine loaded microspheres made of Eudragit RS 100, RL 100 and their combinations. Acta Pol Pharm 68:409–415
27. Danaei M, Dehghankhold M, Ataei S, Hasanzadeh Davarani F, Javanmard R, Dokhani A (2018) Impact of particle size and polydispersity index on the clinical applications of lipidic nanocarrier systems. Pharmaceutics 10:57
28. Adibkia K, Javadzadeh Y, Dastmalchi S, Mohammadi G, Niri FK, Alaei-Beirami M Naproxen– (2011) Eudragit® RS100 nanoparticles: preparation and physicochemical characterization. Colloids Surf B: Biointerfaces 83:155-159
29. Wada R, Hyon S-H, Ikada Y (1990) Lactic acid oligomer microspheres containing hydrophilic drugs. J Pharm Sci 79:919–924
30. Babay D, Hoffman A, Benita S (1988) Design and release kinetic pattern evaluation of indomethacin microspheres intended for oral administration. Biomaterials 9:482–488
31. Kazuhiko J, Masahiro N, Miho K (1986) Controlled release of aclarubicim, an anticancer antibiotic, from poly-β-hydroxybutyric acid microspheres. J Control Release 4:25–32
32. Oh WK, Kim S, Choi M, Kim C, Jeong YS, Cho BR (2010) Cellular uptake, cytotoxicity, and innate immune response of silica-titania hollow nanoparticles based on size and surface functionality. ACS Nano 4:5301–5313
33. Napierska D, Thomassen LC, Rabolli V, Lison D, Gonzalez L, Kirsch-Volders M (2009) Size-dependent cytotoxicity of monodisperse silica nanoparticles in human endothelial cells. Small. 5:846–853
34. Wu T-H, Yen F-L, Lin L-T, Tsai T-R, Lin C-C, Cham T-M (2008) Preparation, physicochemical characterization, and antioxidant effects of quercetin nanoparticles. Int J Pharm 346:160–168
35. Fabbri J, Pensel PE, Albani CM, Arce VB, Mártire DO, Elissondo MC (2019) Drug repurposing for the treatment of alveolar echinococcosis: in vitro and in vivo effects of silica nanoparticles modified with dichlorophen. Parasitology 146:1620–1630
36. Kim DY, Shinde S, Ghodake G (2017) Tuning stable and unstable aggregates of gallic acid capped gold nanoparticles using mg(2+) as coordinating agent. J Colloid Interface Sci 494:1–7
37. Nel A, Xia T, Madler L, Li N (2006) Toxic potential of materials at the nanolevel. Science 311:622–627
38. Ma Q (2013) Role of nrf2 in oxidative stress and toxicity. Annu Rev Pharmacol Toxicol 53:401–426
39. Jiang L, Yu Y, Li Y, Yu Y, Duan J, Zou Y (2016) Oxidative damage and energy metabolism disorder contribute to the hemolytic effect of amorphous silica nanoparticles. Nano Res Lett 11:57
40. Farooq A, Whitehead D, Azzawi M (2014) Attenuation of endothelial-dependent vasodilator responses, induced by dye-encapsulated silica nanoparticles, in aortic vessels. Nanomedicine 9:413–425
41. Guo C, Wang J, Jing L, Ma R, Liu X, Gao L (2018) Mitochondrial dysfunction, perturbations of mitochondrial dynamics and biogenesis involved in endothelial injury induced by silica nanoparticles. Environ Pollut 236:926–936
42. Oprescu AI, Bikopoulos G, Naassan A, Allister EM, Tang C, Park E (2007) Free fatty acid-induced reduction in glucose-stimulated insulin secretion: evidence for a role of oxidative stress in vitro and in vivo. Diabetes 56:2927–2937
43. Ahangarpour A, Heidari H, Mard SA, Hashemitabar M, Khodadadi A (2014) Progesterone and cilostazol protect mice pancreatic islets from oxidative stress induced by hydrogen peroxide. Irania J Pharm Res 13:937
44. Badhani B, Sharma N, Kakkar R (2015) Gallic acid: a versatile antioxidant with promising therapeutic and industrial applications. RSC Adv 5:27540–27557
45. Ferk F, Chakraborty A, Jager W, Kundi M, Bichler J, Misik M (2011) Potent protection of gallic acid against DNA oxidation: results of human and animal experiments. Mutat Res 715:61–71
46. Kuppan G, Balasubramanyam J, Monickaraj F, Srinivasan G, Mohan V, Balasubramanyam M (2010) Transcriptional regulation of cytokines and oxidative stress by gallic acid in human THP-1 monocytes. Cytokine 49:229–234
47. Sameermahmood Z, Raji L, Saravanan T, Vaidya A, Mohan V, Balasubramanyam M (2010) Gallic acid protects RINm5F beta-cells from glucolipotoxicity by its antiapoptotic and insulin-secretagogue actions. Phytother Res 24